Carbohydrate Polymers 82 (2010) 355–362

Contents lists available at ScienceDirect

Carbohydrate Polymers

journal homepage: www.elsevier.com/locate/carbpol

Xyloglucan nano-aggregates: Physico-chemical characterisation in buffer solution and potential application as a carrier for camptothecin, an anti-cancer drug

Tatiane A. Jó[a,d], Denise F.S. Petri[b], Leila M. Beltramini[c], Neoli Lucyszyn[d], Maria Rita Sierakowski[d,*]

[a] Department of Biochemistry and Molecular Biology, Federal University of Paraná, Curitiba, PR, Brazil
[b] Institute of Chemistry, University of São Paulo, São Paulo, SP, Brazil
[c] Institute of Physics of São Carlos, University of São Paulo, São Carlos, SP, Brazil
[d] Laboratory of Biopolymers, Department of Chemistry, Federal University of Paraná, Curitiba, PR, Brazil

ARTICLE INFO

Article history:
Received 10 March 2010
Received in revised form 20 April 2010
Accepted 23 April 2010
Available online 6 May 2010

Keywords:
Xyloglucan
Tamarindus indica
Polysaccharides
Camptothecin
Nano-aggregates
In vitro drug release

ABSTRACT

In this work, native xyloglucan was extracted from *Tamarindus indica* seeds (XGT), and its properties in phosphate buffer solution (PBS) were evaluated in comparison with a commercial tamarind kernel powder (TKP). The physico-chemical characteristics of the polysaccharides such as molar mass, critical concentration and intrinsic viscosity were determined. Furthermore, using spectroscopic and microscopy techniques, it was observed that the XGs tested can be considered macromolecules able to aggregate as nano-entities of 60–140 nm. The XGT tended to an ordered and compact spherical conformation determined by the Huggins constant, circular dichroism, atomic force microscopy and transmission electron microscopy. After the determination of the properties in PBS the XGs, at concentrations of 25% above their critical aggregation concentration, were used to encapsulate camptothecin, an anti-cancer drug. The XGT sample showed an encapsulation efficiency of 42% and first-order drug delivery kinetics. These results demonstrated the importance of knowledge of the physico-chemical properties of polysaccharides, for example, to better conduct their biotechnological applications as drug carriers.

1. Introduction

Polysaccharides are the most important source for a broad variety of advanced polymeric materials and have emerged as an immense renewable resource for biopolymers. These features have led to an outstanding increase in interest among scientists, research institutes and industrial companies (Castro, Silva, Carmona-Ribeiro, Kappl, & Petri, 2007; Heinze et al., 2005; Jelinek & Kolusheva, 2004; Sierakowski, Castro, Lucyszyn, & Petri, 2007; Silva, Carmona-Ribeiro, & Petri, 2007; Ueta & Diniz, 2008).

Polysaccharides are abundant and readily available from renewable sources such as the algal and plant kingdoms, microbial cultures of selected strains and through recombinant DNA techniques. Thus, they have a large variety of compositions and properties that cannot be mimicked easily in the laboratory. Their ease of production makes many polysaccharides cheaper than synthetic polymers (Coviello, Matricardi, Marianecci, & Alhaique, 2007).

The xyloglucans (XGs) are a group of storage or structural heteropolysaccharides from plants, and their structure is composed of a 1,4-linked β-D-glucan main chain that is partially substituted with α-D-Xyl side-chains at the O-6 atoms. Depending on the source, the side-chains can be β-D-Gal-1,2-α-D-Xyl or α-L-Fuc-1,2-β-D-Gal-1,2-α-D-Xyl (Carpita & Gibeaut, 1993; Fry, 1989; Hayashi, 1989; McNeil, Darvill, & Fry, 1984; Varner & Lin, 1989) or more complex chains (Hantus, Pauly, Darvill, Albersheim, & York, 1997; Freitas et al., 2005; Jia, Qin, Darvill, & York, 2003; York, Kumar-Kolli, Orlando, Albersheim, & Darvill, 1996).

The branches present in the structure of xyloglucans may also contribute to the variation in viscosity as well as its solubility and conformational flexibility of the main chain; therefore, different branches may give different properties to the polysaccharide (Sims et al., 1998).

The XGs are water-soluble, but the individual macromolecules tend not to fully hydrate, and, consequently, aggregated species remain present even in very dilute solutions. The biopolymer shows a balance between hydrophobic and hydrophilic character, and the substantial chain stiffness of the cellulose-like backbone facilitates

* Corresponding author. Current address: Laboratório de Biopolímeros, Depto. de Química, Universidade Federal do Paraná, C.P. 19081, Rua Francisco H. dos Santos, s/n°, Centro Politécnico, Curitiba, PR, 81531-990, Brazil, Tel.: +55 41 33613260; fax: +55 41 33613186.
E-mail address: mariarita.sierakowski@ufpr.br (M.R. Sierakowski).

0144-8617/$ – see front matter © 2010 Elsevier Ltd. All rights reserved.
doi:10.1016/j.carbpol.2010.04.072

intermolecular interactions (Nishinari & Takahashi, 2003; Picout, Ross-Murphy, Errington, & Harding, 2003).

Due to its unique rheological properties, the xyloglucans have potential usage in the food (Bhattacharya, Bal, Mukherjee, & Bhattacharya, 1991; Maeda, Yamashita, & Morita, 2007; Yamanaka et al., 2000), pharmaceutical, medical and cosmetic industries (Burgalassi, Panichi, Saettone, Jacobsen, & Rassing, 1996; Itoh et al., 2008), among others.

Another important characteristic of the XGs are that they do not present toxicity (Shirakawa, Yamotoya, & Nishinari, 1998) and can be used, for example, to administer certain drugs. Coviello et al. (2007) indicated that this polysaccharide is a promising protector, especially in the delivery of oral drugs that can be stomach irritants. Furthermore, xyloglucan can also be considered as a suitable polymer for coating nanocomposites of LDH-enalapril (Ribeiro, Arizaga, Wypych, & Sierakowski, 2008), mucoadhesive formulations (Yoo et al., 2005) and for drugs that are administered intraperitoneally (Suisha et al., 1998), rectally (Miyazaki et al., 1998), percutaneously and topically (Takahashi et al., 2002). They are also suitable for ocular applications (Burgalassi, Chetoni, Panichi, Boldrini, & Saettone, 2000; Miyazaki et al., 2001).

Camptothecin (CPT) is a potent cytotoxic alkaloid, which was first isolated and characterised by Wall et al. (1966) from the oriental tree *Camptotheca accuminata*. CPT has a unique mechanism of action as a topoisomerase I inhibitor (Hsiang, Hertzberg, Hecht, & Liu, 1985), and it is believed to act by stabilising a topoisomerase I-induced single strand break in the phosphodiester backbone of DNA, thereby preventing re-ligation, which leads to the production of double-strand DNA breaks during replication and, if not repaired, results in cell death (Hsiang et al., 1985; Liu, 1989). CPT has shown potent antitumour activity against a wide spectrum of human malignancies, including human lung, prostate, breast, colon, stomach and ovarian carcinomas, melanoma, lymphomas and sarcomas (Dancey & Eisenhauer, 1996; Potmesil & Pinedo, 1995; Takimoto, Wright, & Arbuck, 1998).

Therapeutically, CPT has not yet been fully utilised, due primarily to its poor solubility in water and its toxic effects after long administration times (Cortesi, Esposito, Maietti, Menegatti, & Nastruzzi, 1997). Attempts to deliver CPT or its derivatives efficiently have included encapsulation in microspheres, microemulsions, polymeric micelles and polymeric implants (Cortesi et al., 1997; Hatefi & Amsden, 2002; Shenderova, Burke, & Schwendeman, 1997, 1999; Storm et al., 2002).

In the present paper, we determined the physico-chemical properties of two samples of tamarindus xyloglucans (XGs) in phosphate buffer solution (PBS) by observing the aggregation characteristics, and, after this analysis, the XG solutions were tested to load and release CPT *in vitro*.

2. Materials and methods

2.1. Materials

A xyloglucan sample (coded XGT) was extracted from tamarind (*Tamarindus indica*) seeds from a market in the State of Rio Grande do Norte, Brazil and compared with a commercially available xyloglucan (coded TKP, i.e., Tamarind kernel powder) that was obtained from Balasanka Mills Co., India. We measured molar ratios of the Glc:Xyl:Gal units of 2.8:2.3:1 (XGT) and 2:2:1 (TKP) by ^{1}H NMR spectroscopy, using a Bruker Avance DRX-400 spectrometer. D_2O was used as the solvent, and the experiments were carried out at 70 °C. The chemical shifts are reported as δ (ppm) relative to acetone (δ 2.224), which was used as an internal standard. Other XG characterisation parameters have already been reported (Jo, Petri, Valenga, Lucyszyn, & Sierakowski, 2009). Camptothecin (CPT; $C_{20}H_{16}N_2O_4$, M_w = 348.4 g/mol) was purchased from Sigma–Aldrich. The other materials were of commercial grade and were used without purification.

2.2. Analysis of the xyloglucan. Its polydispersity, molar mass and critical concentration

After aqueous extraction, the samples (1 mg/mL) were solubilised in pure MilliQ water and filtered through 0.45 and 0.22 μm pore cellulose acetate membranes. The solutions (100 μL) were measured using GPC to calculate the polydispersity index ($\overline{M}_w/\overline{M}_n$) and the molar mass, $\overline{M}_w$, relative to PEO 22k (polyethylene oxide) and Dextran 70k, which were used as standards. The samples were analysed at 632.8 nm using a Viscotek system equipped with PWxl 6000, 4000 and 2500 columns (Tosoh, Japan) that were connected in series, which was coupled to a differential refractometer from Viscotek (model VE3580), a viscosimetric detector and a laser light scattering detector (model 270 Dual Detector). The setup was also equipped with low angle (7°) and right angle (90°) lasers, and the sample was eluted with pure MilliQ water at a flow rate of 1 mL/min. By determining the $\overline{M}_w$, it was possible to calculate the critical concentration (c^*), which determines the limit concentration between the diluted and semi-diluted states, using Eq. (1):

$$c^* = \frac{\bar{M}_w}{(4/3)\pi \times NA \times {R_g}^3} \quad (1)$$

where $\overline{M}_w$ is the molar mass (g/mol), NA is Avogadro's constant, and R_g is the radius of gyration (nm). The values calculated using Eq. (1) were comparable with those found using rheological analysis.

2.3. Rheological measurements

For the intrinsic viscosity determinations, we solubilised the XG samples (1.2–0.6 g/L) in PBS (28 mM phosphate buffer solution containing 123 mM NaCl, at pH 7.4) to simulate physiological conditions (Ciccoli, Signorini, Alessandrini, Ferrali, & Comporti, 1994; Ferrali et al., 1997). We used the Huggins equation to determine the intrinsic viscosity ([η]) by extrapolation of the reduced viscosity (η_{red}) to the limit at zero concentration ($c \to 0$), where the linear coefficient is represented by [η] (Huggins, 1942). All of the analyses were performed using a RheoStress1 rheometer (Haake GmbH, Germany) equipped with a DG43 spindle. A Haake DC30 bath and a thermostatic Universal Temperature Controller (UTC) were used to maintain the temperature at 25 °C.

2.4. Conformational analysis

The circular dichroism (CD) spectra were recorded over the range of 190–250 nm (measured in millidegrees (mdeg) on a Jasco J-815 spectropolarimeter (Jasco Instruments, Japan). We recorded the average of 16 scans using a 0.1 cm path length cylindrical quartz cuvette and a sample concentration of 1.0 mg/mL. The entire instrument, including the sample chamber, was constantly flushed with N_2 gas during operation. The spectra were obtained after overnight stirring (approximately 20 h of incubation in PBS). Spectra were recorded at 5, 25 and 37 °C, and the temperatures were maintained using a circulating water bath TC-100 (Jasco). At each temperature tested, the sample was incubated for 5 min before the analysis.

2.5. Determination of the critical aggregation concentration of the polysaccharides. Fluorescence measurements.

To compare the encapsulating capacity of the polysaccharides (Amiji, 1995), the samples were diluted in PBS at concentrations from 0.001 to 2.0 mg/mL. Pyrene, dissolved in methanol, was added

Table 1
The solution properties of tamarind (XGT) and commercial xyloglucan (TKP).

Samples	$\bar{M}_w$[a] (g/mol)	R_g[a] (nm)	R_h[a] (nm)	c^*[a] (mg/mL)	c^*[b](mg/mL)	$[\eta]_d$[a] (mL/g)	$[\eta]_r$[c](mL/g)	α[a]
XGT	653,000	57.3	33.2	1.38	1.3	360.5	609.4	0.13
TKP	803,000	59.9	41.1	1.48	1.2	592.9	359.8	0.44

Symbols used: molar mass ($\bar{M}_w$), the radius of gyration (R_g), the hydrodynamic radius (R_h); the critical concentration (c^*), the intrinsic viscosity (η) and the Mark–Houwink constant (α).

[a] Measured using GPC, Viscotek 270 Dual Detector (RI, viscosity. LALS and RALS detectors), columns PWxl 2500, 4000 and 6000.

[b] Measured using the Rheometer, Haake RS 1, sensor DG 43, at 25 °C.

[c] Measured using rheology

to the XG solution to a final concentration of 2.0 μM. The excimer emission spectra were obtained using a F4500 fluorescence spectrophotometer (Hitachi, Japan) and a 1 cm path length quartz cuvette. The probe was excited at 343 nm, and the emission spectrum was collected in the range 360–430 nm at a scan speed of 60 nm/min. The excitation and emission slit openings were 5.0 and 1.0 nm, respectively. The III/I ratio (at 373 and 383 nm, respectively) has been used to study the change in the environmental polarity of amphipathic molecules on association in aqueous solutions (Dualeh & Steiner, 1990). For example, Kalyanasundaram and Thomas (1977) used the III/I ratio to determine the critical micelle concentration (CMC), also called the critical aggregation concentration (CAC).

2.6. Microscopy imaging of thin films

Atomic force microscopy (AFM) imaging was performed at room temperature (25 °C) using a commercial SPM-9500J3 microscope (Shimadzu Co., Japan). We took 2 μm × 2 μm images in the dynamic tapping mode (TM-AFM) using an oxide-sharpened microfabricated silicon μ-Masch cantilever (Estonia), with a nominal spring constant of 4.7 N/m and a tip radius of curvature of less than 10 nm. The scanning rate was 1 Hz, and 256 × 256 data points were acquired. The image data were flattened and then noise-filtered when necessary. The operating point was adjusted to minimise the interaction between the tip and the sample to avoid soft layer deformation. The samples were diluted in PBS using the concentration measurements that were determined using fluorescence and stirred overnight for approximately 18 h at 25 °C. Then, silicon wafers (1 cm × 1 cm) were dipped for 24 h into homogenous solutions, washed with pure MilliQ water and dried at 25 °C under conditions where the humidity was controlled (40%). The equipment software was used to treat the images and analyse the topography. It was possible to observe the homogeneity of the surface, the size and aggregation of the particles and the roughness using the rms values.

We obtained TEM micrographs using a JEOL 1200EX-II transmission electron microscope. We adsorbed the same concentration as was used for the AFM measurements (5 μL of each XG solution in PBS) onto a copper grid that was coated with a parlodium/carbon film. The drops were dried overnight under controlled temperature (20 °C) and moisture (40%) before the measurements.

2.7. Preparation and analysis of the xyloglucan solution to load camptothecin

The samples in PBS were prepared in duplicate based on the experimental observations of Aiping, Jianhong, and Wenhui (2006), which suggested that the samples be solubilised at a concentration of 25% above the CAC (as determined using pyrene as a probe). After overnight stirring (approximately 20 h), we added camptothecin (40% (w/w) of the XG weight) according to Opanasopit et al. (2006) and Watanabe et al. (2006). Furthermore, the mixture was stirred for approximately 48 h and then centrifuged at 5922 × *g* for 30 min at 25 °C to eliminate the drug that was not loaded. For the drug loading analysis, we compared the absorbance of the XG–CPT complexes that were formed against a standard curve of CPT in PBS diluted in 1 M NaOH. The absorbance was measured using a spectrophotometer (SP 220, Biospectro, Brazil) and a 1 cm path length quartz cuvette at 369 nm. The fluorescence was analysed to confirm the encapsulation of CPT into the XG branches by excitation at 343 nm and acquiring the emission spectrum in the range of 375–600 nm (Liu & Li, 2005). The scan speed and slit widths were the same as those used for the earlier fluorescent measurements.

2.8. In vitro drug release study

The *in vitro* release study was based on the report by Xiong, Tam, and Gan (2005), as adapted by Aiping et al. (2006). Briefly, 3 mL of XG-CPT and CPT aqueous saturated solution was placed in a dialysis membrane (molecular weight cut-off: 12,000–16,000 g/mol, average pore size: 2.5 nm). The sealed dialysis membrane was placed in PBS at pH 7.4 (100 mL). The container was then placed into a stirred water bath at 37 °C for the drug release study. At predetermined time intervals, the CPT solution that was released outside the dialysis membrane was withdrawn (3 mL) and measured at 369 nm to determine the concentration of CPT. Fresh PBS (3 mL) was added to replenish the sample that was removed to maintain a constant volume. The drug release experiments were performed in duplicate.

3. Results and discussion

3.1. Characterisation of the xyloglucan solution

Some of the basic analyses of the polysaccharides have already been reported (Jo et al., 2009), and others are shown and discussed in this work. First, we determined the critical concentration (c^*, Table 1) to analyse the behaviour of the macromolecules in the diluted solution without polymer–polymer interference, in other words, under conditions in which polymer aggregation would not occur. The value of c^* was calculated using rheology by plotting $\log \eta_{sp}$ as a function of $\log C \times [\eta]$ and using Eq. (1), which relates the values of $\overline{M}_w$ and R_g. The calculated concentrations were very similar using both techniques, as molecular aggregation causes less interference with the solution viscosity using rheology than when using GPC, which is more sensitive. The intrinsic viscosities $[\eta]$ of XGT and TKP were determined graphically (Fig. 1) as 609.4 and 359.8 mL/g, respectively. These values were lower than the relevant values for *Detarium senegalenses* (890 mL/g) (Wang, Ellis, Ross-Murphy, & Reid, 1996) and *Hymenaea courbaril* (971 mL/g) (Lucyszyn et al., 2009) and were similar to that for *T. indica* (Freitas et al., 2005). The differences are probably due to different extraction processes used and origin of the seeds. We calculated the Huggins constant (Huggins, 1942), k', to be 0.28 for XGT and 0.51 for TKP, and therefore $0.8 < k' < 0.3$; thus, the solvent used can be considered favourable to polymer–solvent interactions. It is important to determine and establish the macromolecular characteristics of the polysaccharide for its applications, and linking size exclusion chromatography to laser light scattering is an excellent option

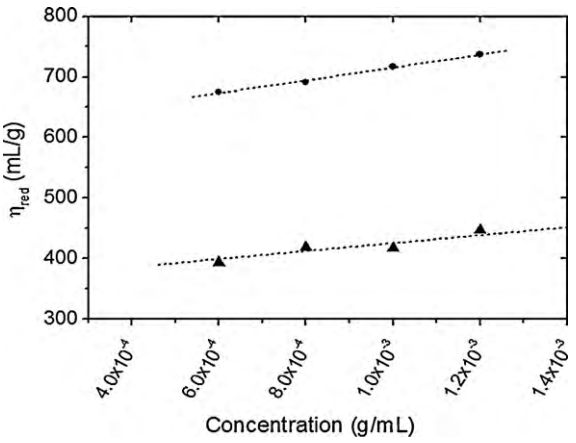

Fig. 1. Determination of the intrinsic viscosity [η] (mL/g) for tamarind (XGT, ●) and commercial xyloglucan (TKP, ▲) in PBS (pH 7.4) at 25 °C.

because it is fast and requires small amounts of the sample. After solubilisation and ultrafiltration, samples eluted between 9 and 12 mL showed polydisperse profiles with values more accentuated to TKP (1.21) than XGT (1.05). These values can affect the [η] that is measured using GPC and rheology. The average molar masses of XGT and TKP determined were similar to each other: 6.53×10^5 and 8.03×10^5 g/mol, respectively. The R_g values were calculated as 57.3 and 59.9 nm for XGT and TKP, respectively (Table 1). The high M_W was frequently observed using different seed sources of XG, such as *H. courbaril* (7.0×10^5) (Lucyszyn et al., 2009), *T. indica* ($\sim 1.1 \times 10^6$) (Freitas et al., 2005), *Afzelia africana* (8.2×10^5) (Ren, Picout, Ellis, Ross-Murphy, & Reid, 2005) and *Copaifera langsdorffii* (7.8×10^5) (Stupp et al., 2008). We observed that the dimensions of the macromolecules can also vary according to the behaviour of the molecule in solution, depending on the solubilisation time and polymer–solvent interactions (Freitas et al., 2005). Generally, if $0 < \alpha < 0.5$, then the molecule is considered sphere-like, as was seen with XGT. Values of $0.5 < \alpha < 0.8$ are found for flexible chains or random coil conformations, as obtained with TKP. If $0.8 < \alpha < 1.0$, the molecules tend to be rigid and rod-like.

The XGs were analysed using circular dichroism (CD) to investigate the conformation of the chain. We analysed the spectra from 190 to 250 nm, as shown in Fig. 2, because polysaccharide bands are typically found from 194 to 240 nm (Synytsya, Synytsya, Blafkova, Volka, & Král, 2007). In addition to the widespread use of CD in the study of the secondary structures of proteins, it has also been used to study the conformations of polysaccharides such as ι- and λ-type carrageenans (Schoeler et al., 2006), κ-carrageenans (Nickerson, Paulson, & Hallet, 2004), alginate (Al-Khouri, 2003) and chitosan (Synytsya et al., 2007). Although carbohydrates cannot form defined structures such as the α-helix or β-sheets found in proteins, they can exist as disordered chains, as extended rigid chains (as in cellulose) or as collapsed, flexible, helix-like chains (as in amylose). We analysed purified samples to minimise the protein content, which can affect the spectrum. Using the results presented, it was possible to note little or no influence of temperature on the conformation of TKP (Fig. 2B). XGT (Fig. 2A) was influenced more, as was seen by comparing the signals at 5 °C with those at 25 and 37 °C: different peaks were seen at 5 °C than at the other temperatures tested, with a maximum at 198 nm and minima at 208 and 220 nm, indicating the influence of helix-like structures. At higher temperatures, i.e., at 25 and 37 °C, the maximum peak was displaced to approximately 202 nm, and the minimum was displaced to 220 nm, indicating a greater contribution from sheet-like structures, i.e., indicating chain extension. The ordered structure of XGT might contain a helical structure, leading to a more compact chain at 5 °C, and it can contain sheet-like structure at 25 and 37 °C, or a more extended chain, which probably has an effect on the viscosity in solution. The viscosity of XGT (609.4 mL/g) was higher than that of TKP (359.8 mL/g). Similar behaviour was observed in the carrageenans (Schoeler et al., 2006); in solution, the λ-type presents a random coil conformation and was not able to form a gel, whereas the ι-type adopted a helix-like conformation, conferring higher viscosity to the solution. The results from the CD analysis agreed with the observations made using GPC, and both indicated that XGT tended to an ordered and compact conformation. The helix- and sheet-like elements that were determined using CD and the value of the Mark–Houwink α-constant suggested a compact structure like a sphere. TKP could be defined as a flexible chain with a random coil conformation when both techniques were compared.

3.2. Determination of the critical encapsulating concentration of XG. Fluorescence measurements

Because pyrene is a hydrophobic molecule and has low water solubility (approximately 0.3 μM), it was expected to prefer the hydrophobic domains of amphipathic molecules (Dowling & Thomas, 1990). The fluorescence emission spectrum of pyrene is sensitive to the polarity of the medium in which it is dispersed, and thus the intensity of the band I peak (373 nm) increases in the presence of polar solvents, and the intensity of the band III peak (383 nm) increases in non-polar solvents. The relationship between bands III and I can be altered when the polarity of the system varies. For macromolecules, this change may indicate that conformational changes have taken place in the molecule. For this and other reasons, this methodology is used to study polymer behaviour in solution (Kalyanasundaram & Thomas, 1977; Vieira, Moscardini, Tiera, & Tiera, 2003).

Constructing a graph of intensity of fluorescence emission as a function of the increasing concentration of XGT (data not shown), it was possible to determine the value of the critical aggregation con-

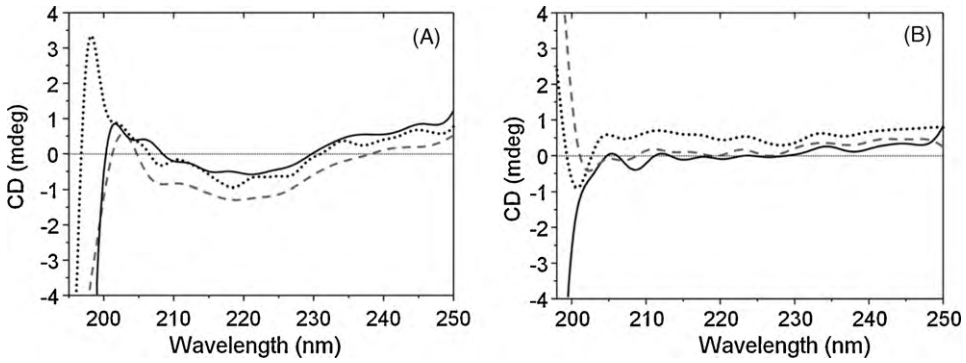

Fig. 2. Circular dichroism spectra of the polysaccharides at 1 mg/mL in PBS: at 5 °C (dotted line), 25 °C (solid line) and 37 °C (dashed line). (A) XGT and (B) TKP.

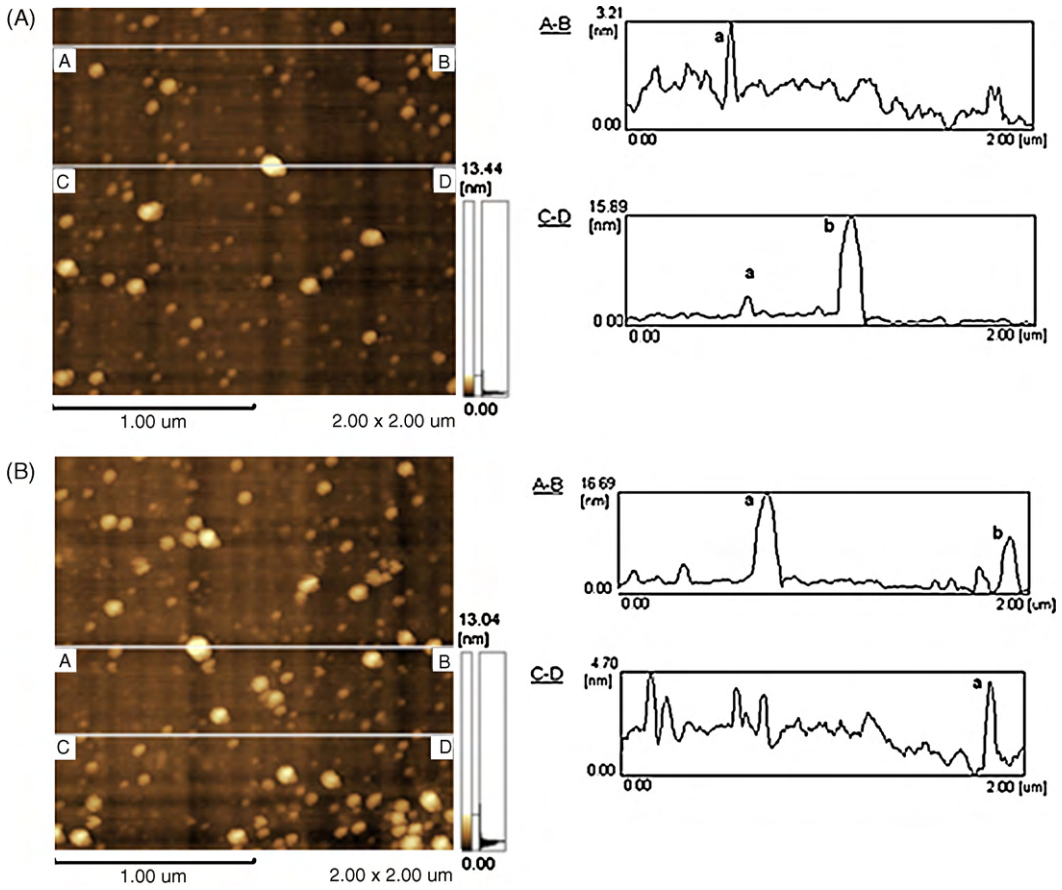

Fig. 3. An image of the topography of the xyloglucans from (A) the native tamarind (XGT) and (B) commercial (TKP) solutions deposited onto a silicon surface at the critical aggregation concentration in PBS (pH 7.4).

centration (i.e., the CAC) (Amiji, 1995) as 0.038 mg/mL. The value for TKP was 0.09 mg/mL. The study of pyrene incorporation in polymer solutions can be used as a model for the interaction with hydrophobic drugs, and further studies of the effective encapsulation and release of drugs *in vitro* were based on those proposed by Xiong et al. (2005).

3.3. Atomic force microscopy and transmission electron microscopy analysis

From the critical aggregation concentration in solution (CAC), after adsorption of XG on the silicon wafers as substrate, the particle aggregates and fibres were visualised by atomic force microscopy in the dynamic mode in a corresponding area of 2 μm × 2 μm, as shown in Fig. 3. By treating the images, it was possible to determine the approximate size (width) of certain particles and their height, as well as the rms that was used to compare the roughness of the surfaces.

The sections shown in the images (Fig. 3) indicated that all of the samples were able to form nanoparticles or nano-aggregates, i.e., small spherical bodies from 60 to 190 nm. The quite diverse height of the spheres may suggest overlapped entities, and these were also noticed in the TEM images (Fig. 4). XGT had a lower rms value (1.049 nm), indicating that it had a flatter surface than TKP (rms = 1.457 nm) (Kosaka, Koawan, Salvadori, & Petri, 2005). Looking at the AFM images (Fig. 3), we observed that the morphologies of different XGs were very similar (the polysaccharides are the clearer entities on the top of the image).

We observed the morphologies of the XGs samples using transmission electron microscopy. The images showed that spherical particles were arranged in clusters, which were very similar for the two XGs. However, the sizes ranged from 14 to 50 nm (Fig. 4). The presence of such clusters complemented the AFM data, which showed small spherical entities of diverse sizes and heights that confirm the presence of overlapping molecules.

3.4. Preparation and analysis of the XG encapsulating complexes

We performed encapsulating and *in vitro* release assays using camptothecin (CPT) solubilised in PBS or in PBS containing XGs.

First, we prepared solutions of XG in PBS. Then, we added 40% (w/w) of camptothecin to the xyloglucan solution (Opanasopit et al., 2006; Watanabe et al., 2006). The system was stirred for 48 h and centrifuged. The encapsulation efficiency was then determined using UV–vis spectroscopy for further *in vitro* release. The XGs had encapsulation efficiencies of 29% (TKP) and 42% (XGT).

Camptothecin in saline buffer solution was released *in vitro* in polymer solutions containing xyloglucans at concentrations 25% above their critical aggregation concentration (CAC). This was based on the study of Aiping et al. (2006), who observed that when using O-carboxymethylchitosan (OCMCS), the efficiency of the encapsulation of camptothecin was greater when using a concentration that was slightly higher than the CAC that had been determined for the polymer. According to their study, this result occurred because, although there are no aggregates in solution below the CAC, hydrophobic interactions and hydrogen linkages may exist between the polymeric chains and camptothecin due to the amphiphilic character of the OCMCS derivative. The same authors explained that this type of interaction may facilitate the solution of CPT in the OCMCS solution, and hydrophobic molecules

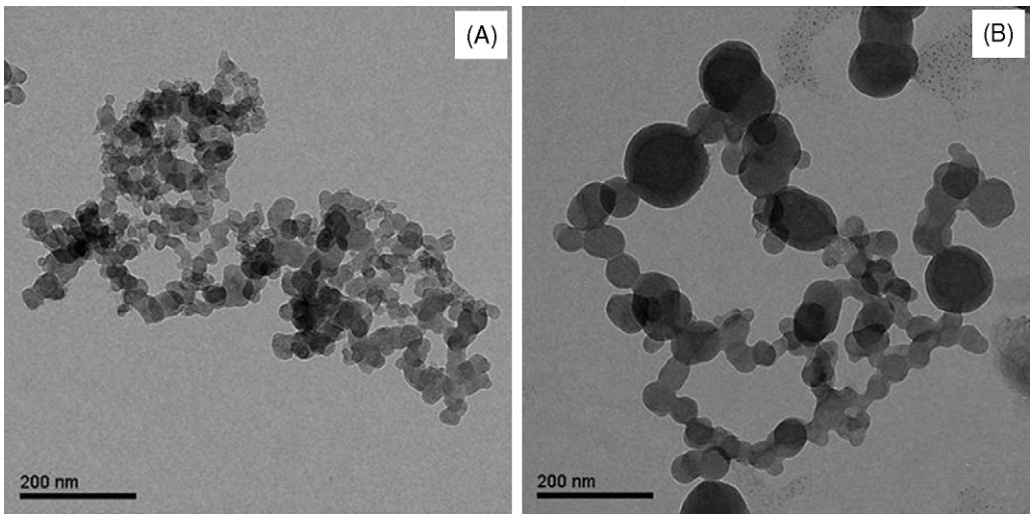

Fig. 4. Transmission electron microscopy images. (A) XGT, enlargement: 150,000× and (B) TKP, enlargement: 150,000×. These were tested at their critical aggregation concentration (mg/mL) in PBS (pH 7.4).

and drugs can be solubilised in the core of the aggregates at the CAC. However, at concentrations much greater than the CAC more compact clusters are formed, and these clusters capture a much smaller quantity of the drugs, which indicates that not only were the aggregates able to increase the solubility of camptothecin, a hydrophobic molecule, but also the chain was able to accomplish the same feat alone. Nishinari and Takahashi (2003) have reported that even the native XG of tamarind seeds has a balanced hydrophobic and hydrophilic character, facilitating the intermolecular interactions and consequently allowing the encapsulation of hydrophobic molecules inside the chain or the nucleus (also called the "core"). To ensure that camptothecin was localised in the polymer core, we compared the fluorescence emission spectrum of camptothecin in XG solutions (excitation at 369 nm) to solutions of camptothecin alone in PBS (data not shown).

3.5. *In vitro* CPT release study

The *in vitro* release assay showed that all of the samples that contained xyloglucan promoted a slower release of drug than when camptothecin was dissolved alone in the PBS, in a very similar manner (Fig. 5).

In the absence of XG, 100% of the camptothecin was quickly released after 3.5 h. However, the solutions that contained XG sustained the release and prolonged it for up to 24 h (Table 2). At this time, the drug was not yet released completely.

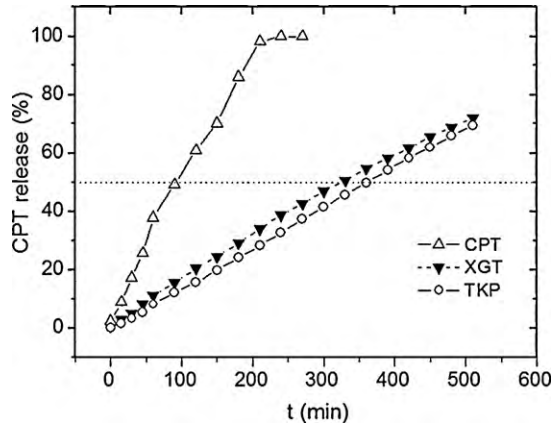

Fig. 5. The *in vitro* release of camptothecin alone into PBS (CPT), and when used in the presence of the xyloglucan nano-aggregates tamarind (XGT) and commercial (TKP) in PBS (pH 7.4). The dotted lines are drawn as guides for the eyes.

When we analysed the collected data (Table 2), we observed that approximately 75% of the drug was released, even after 24 h, which means that the drug loaded with xyloglucan was not fully released after the one-day test. The time required to release half of the encapsulated drug was much higher (at least 314 min) than when camptothecin was solubilised in PBS (93 min) in the absence of XG.

On average, the solutions of XG that we tested prolonged the release for 244 min (almost 4 h). The sample that contained XGT was effective in prolonging the release of camptothecin with a higher encapsulation efficiency (42%) and slower release rate than when camptothecin was used alone in saline buffer solution and when it was combined with commercial xyloglucan from tamarind kernel powder. Even so, at the lowest CAC this means a small amount of polymer was required to encapsulate the drug.

Generally, the kinetics of drug release from polymeric micelles is affected by several factors including the particle size, block composition, molecular weight, concentration and degradation rate (Kim, Ha, & Lee, 2000). The release mechanism can be categorised as diffusion controlled, degradation controlled or a mix of the two (Siepmann & Peppas, 2001; Zuleger & Lippold, 2001).

When the fraction of drug released is lower than 0.85, the Bhaskar equation (Eq. (2)) can be used to evaluate whether diffusion through the particle is the rate-limiting step. The other equation that can be used is the first-order equation (Eq. (3)), which is normally used to describe dissolution phenomena (Ambrogi, Fardella, Grandolini, Perioli, & Tiraldi, 2002).

$$-\log(1-X) \text{ versus } t^{0.65} \quad (2)$$

$$-\log(1-X) \text{ versus } t \quad (3)$$

where X is the released fraction within the release time t.

Table 2
The release of camptothecin *in vitro* into the buffer solution (PBS) when used alone and when used in different xyloglucan solutions: the released fraction after 24 h ($F_{24\,h}$) and the time required to release 50% of the drug ($t_{50\%}$).

Saturated CPT into	$F_{24\,h}$ (%)	$t_{50\%}$ (min)
PBS	100[a]	93
XGT	75.7 ± 12.6	314
TKP	73.2 ± 0.4	350

[a] Fully released after 210 min.

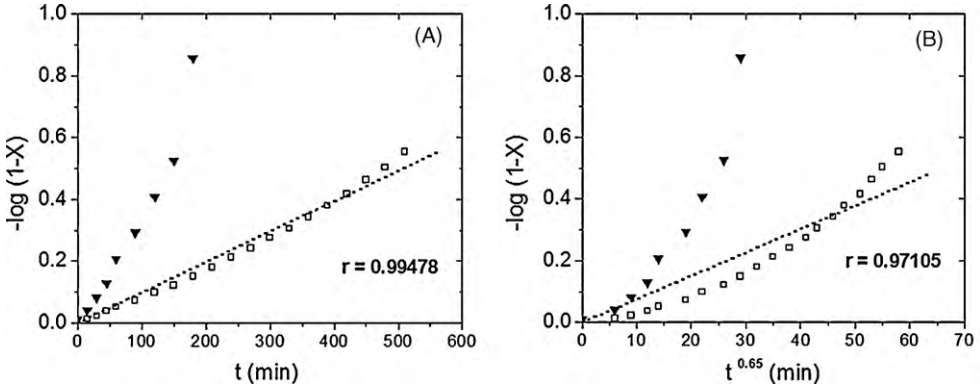

Fig. 6. The release of camptothecin alone into PBS (▼) and into XGT nano-aggregates (□); the data were fitted using different kinetic models: (A) a first-order model and (B) the Bhaskar model.

The results of the kinetic models are shown in Fig. 6 for the best polysaccharide tested, XGT. Using the first-order model shown in Fig. 6A, the correlation factor of linear regression was 0.995, and the linear correlation in the Bhaskar model was 0.971 (Fig. 6B). We observed that the release of camptothecin fit better to the first-order equation than to the Bhaskar equation. These results can be explained by reference to Zhang, Zou, Guo, and Duan (2006), who discussed the possibility of the dissolution of the polymer in the buffer solution and then drug release.

4. Conclusions

In physico-chemical characterisation of two xyloglucans samples obtained from tamarind seeds (native and commercial) in phosphate buffer solution, it was observed that the XGT (native tamarind xyloglucan) took a spherical form, as confirmed by several methods, forming nano-aggregates of 60 nm as determined by atomic force microscopy analysis. Applying XGT for *in vitro* experiments, at a concentration 25% above the critical concentration, 42% efficiency for encapsulation and sustained release of camptothecin was demonstrated. The promising results showed that the knowledge and the control of the physico-chemical behaviour of xyloglucans in solution are important for biotechnological applications.

Acknowledgements

The authors acknowledge all the collaborators and Brazilian funding agencies, including CNPq (Conselho Nacional de Pesquisa), CAPES-Brasil and Fundação Araucária, for financial support and CME/UFPR, DFIS/UFPR, DQUI/UFPR for analysis support. The authors are also grateful to Dr. Vadakkethonippurathu Sivankutty Nair Prasad for collaboration and Balasanka Mills (India) for providing the TKP sample.

References

Aiping, Z., Jianhong, L., & Wenhui, Y. (2006). Effective loading and controlled release of camptothecin by O-carboxymethylchitosan aggregates. *Carbohydrate Polymers*, *63*, 89–96.

Al-Khouri, I. S. (2003). UV/VIS and CD spectral studies of the interaction between pinacyanol chloride and alginates, γ-cyclodextrin, and aerosol-OT. PhD thesis, Germany: Universität Duisburg.

Ambrogi, V., Fardella, G., Grandolini, G., Perioli, L., & Tiraldi, M. C. (2002). Intercalation compound of hydrotalcite-like anionic clay with anti-inflammatory agents. II. Uptake of diclofenac for a controlled release formulation. *AAPS PharmSciTech*, *3*, 26. Available at:. http://www.aapspharmscitech.org/

Amiji, M. M. (1995). Pyrene fluorescence study of chitosan association in aqueous solution self. *Carbohydrate Polymers*, *26*, 211–213.

Bhattacharya, S., Bal, S., Mukherjee, R. K., & Bhattacharya, S. (1991). Rheological behaviour of tamarind (*Tamarindus indica*) kernel powder (TKP) suspension. *Journal of Food Engineering*, *13*, 151–158.

Burgalassi, S., Chetoni, P., Panichi, L., Boldrini, E., & Saettone, M. F. (2000). Xyloglucan as a novel vehicle for timolol: Pharmacokinetics and pressure lowering activity in rabbits. *Journal of Ocular Pharmacology and Therapeutics*, *16*, 497–509.

Burgalassi, S., Panichi, L., Saettone, M. F., Jacobsen, J., & Rassing, M. R. (1996). Development and in vitro/in vivo testing of mucoadhesive buccal patches releasing benzydamine and lidocaine. *International Journal of Pharmaceutics*, *133*, 1–7.

Carpita, N. C., & Gibeaut, D. M. (1993). Structural models of primary cell walls in flowering plants: Consistency of molecular structure with the physical properties of the cell wall during growth. *The Plant Journal*, *3*, 1–30.

Castro, L. B. R., Silva, F. F., Carmona-Ribeiro, A.-M., Kappl, M., & Petri, D. F. S. (2007). Immobilization of hexokinase onto chitosan decorated particles. *Journal of Physical Chemistry B*, *111*, 8520–8526.

Ciccoli, L., Signorini, C., Alessandrini, C., Ferrali, M., & Comporti, M. (1994). Iron release, lipid peroxidation and morphological alterations of erythrocytes exposed to acrolein and phenylhydrazine. *Experimental and Molecular Pathology*, *60*, 108–118.

Cortesi, R., Esposito, E., Maietti, A., Menegatti, E., & Nastruzzi, C. (1997). Formulation study for the antitumor drug camptothecin: Liposomes, micellar solutions and a microemulsion. *International Journal of Pharmaceutics*, *159*, 95–103.

Coviello, T., Matricardi, P., Marianecci, C., & Alhaique, F. (2007). Polysaccharide hydrogels for modified release formulations. *Journal of Controlled Release*, *119*, 5–24.

Dancey, J., & Eisenhauer, E. A. (1996). Current perspectives on camptothecins in cancer treatment. *British Journal of Cancer*, *74*, 327–338.

Dowling, K. C., & Thomas, J. K. (1990). A novel micellar synthesis and photophysical characterization of water-soluble acrylamide–styrene block copolymers. *Macromolecules*, *23*, 1059–1064.

Dualeh, A. J., & Steiner, C. A. (1990). Hydrophobic microphase formation in surfactant solutions containing an amphiphilic graft copolymer. *Macromolecules*, *23*, 251–255.

Ferrali, M., Signorini, C., Caciotti, B., Sugherinil, L., Ciccoli, L., Giachetti, D., et al. (1997). Protective against oxidative damage of erythrocyte membrane by the flavonoid quercetin and its relation to iron chelating activity. *FEBS Letters*, *416*, 123–129.

Freitas, R. A., Martin, S., Santos, G. L., Valenga, F., Buckeridge, M. S., Reicher, F., et al. (2005). Physico-chemical properties of seed xyloglucans from different sources. *Carbohydrate Polymers*, *60*, 507–514.

Fry, S. C. (1989). The structure and functions of xyloglucan. *Journal of Experimental Botany*, *40*, 1–11.

Hantus, S., Pauly, M., Darvill, A. G., Albersheim, P., & York, W. S. (1997). Structural characterization of novel L-galactose-containing oligosaccharide subunits of jojoba seed xyloglucans. *Carbohydrate Research*, *304*, 11–20.

Hatefi, A., & Amsden, B. (2002). Camptothecin delivery methods. *Pharmacological Research*, *19*, 1389–1399.

Hayashi, T. (1989). Xyloglucan in the primary cell wall. *Annual Review of Plant Physiology and Plant Molecular Biology*, *40*, 139–166.

Heinze, T., Barsett, H., Ebringerová, A., Harding, S. E., Hromádková, Z., Muzzarelli, C., Muzzarelli, R. A. A., et al. (2005). Structure, characterization and use. In *Polysaccharides I* Advances in Polymer Sciences. Berlin: Springer-Verlag.

Hsiang, Y. H., Hertzberg, R., Hecht, S., & Liu, L. F. (1985). Camptothecin induces protein-linked DNA breaks via mammalian DNA topoisomerase I. *The Journal of Biological Chemistry*, *260*, 14873–14888.

Huggins, M. L. (1942). The viscosity of dilute solutions of long chain molecules. IV. Dependence on concentration. *Journal of the American Chemical Society*, *64*, 2716–2718.

Itoh, K., Yahaba, M., Takahashi, A., Tsuruya, R., Miyazaki, S., Dairaku, M., et al. (2008). *In situ* gelling xyloglucan/pectin formulations for oral sustained drug delivery. *International Journal of Pharmaceutics*, *356*, 95–101.

Jelinek, R., & Kolusheva, S. (2004). Carbohydrate biosensors. *Chemical Reviews*, *104*, 5987–6015.

Jia, Z., Qin, Q., Darvill, A. G., & York, W. S. (2003). Structure of xyloglucan produced by suspension-cultures tomato cells. *Carbohydrate Research*, *338*, 1197–1208.

Jo, T. A., Petri, D. F. S., Valenga, F., Lucyszyn, N., & Sierakowski, M.-R. (2009). Thin films of xyloglucans for BSA adsorption. *Material Science and Engineering C*, *29*, 631–637.

Kalyanasundaram, K., & Thomas, J. K. (1977). Environmental effects of vibronic band intensities in pyrene monomer fluorescence and their application in studies of micellar systems. *Journal of the American Chemical Society*, *99*, 2039–2044.

Kim, S. Y., Ha, J. C., & Lee, Y. M. (2000). Poly(ethylene oxide)-poly(propylene oxide)-poly(ethylene oxide)/poly(ε-caprolactone) (PCL) amphiphilic block copolymeric nanospheres. II. Thermo-responsive drug release behaviors. *Journal of Controlled Release*, *65*, 345–358.

Kosaka, P. M., Koawan, Y., Salvadori, M. C., & Petri, D. F. S. (2005). Characterization of ultrathin films of cellulose esters. *Microscopy and Microanalysis*, *11*, 94–97.

Liu, J., & Li, L. (2005). SDS-aided immobilization and controlled release of camptothecin from agarose hydrogel. *European Journal of Pharmaceutical Sciences*, *25*, 237–244.

Liu, L. F. (1989). DNA topoisomerase poisons as antitumor drugs. *Annual Review of Biochemistry*, *58*, 351–375.

Lucyszyn, N., Lubambo, A. F., Matos, K. F., Marvilla, I., Souza, C. F., & Sierakowski, M.-R. (2009). Specific modification of xyloglucan from *Hymenaea courbaril* seeds. *Material Science and Engineering C*, *29*, 552–558.

Maeda, T., Yamashita, H., & Morita, N. (2007). Application of xyloglucan to improve the gluten membrane on breadmaking. *Carbohydrate Polymers*, *68*, 658–664.

McNeil, M., Darvill, A. G., & Fry, S. C. (1984). Structure and function of the primary cell walls of plants. *Annual Review of Biochemistry*, *53*, 625–663.

Miyazaki, S., Suisha, F., Kawasaki, N., Shirakawa, M., Yamatoya, D., & Attwood, D. (1998). Thermally reversible xyloglucan gels as vehicles for rectal drug delivery. *Journal of Controlled Release*, *56*, 75–83.

Miyazaki, S., Suzuki, S., Kawasaki, N., Endo, K., Takahashi, A., & Attwood, D. (2001). In situ gelling xyloglucan formulations for sustained release ocular delivery of pilocarpine hydrochloride. *International Journal of Pharmaceutics*, *229*, 29–36.

Nickerson, M. T., Paulson, A. T., & Hallet, F. R. (2004). Dilute solution properties of κ-carrageenan polysaccharides: Effect of potassium and calcium ions on chain conformation. *Carbohydrate Polymers*, *58*, 25–33.

Nishinari, K., & Takahashi, R. (2003). Interaction in polysaccharide solutions and gels. *Current Opinion in Colloid and Interface Science*, *8*, 396–400.

Opanasopit, P., Ngawhirunpat, T., Chaidedgumjorn, A., Rojanarata, T., Apirakaramwong, A., Phongying, S., et al. (2006). Incorporation of camptothecin into N-phthaloyl chitosan-g-mPEG self-assembly micellar system. *European Journal of Pharmaceutics and Biopharmaceutics*, *64*, 269–276.

Picout, D. R., Ross-Murphy, S. B., Errington, N., & Harding, S. E. (2003). Pressure cell assisted solubilization of xyloglucans: Tamarind seed polysaccharide and detarium gum. *Biomacromolecules*, *4*, 799–807.

Potmesil, M., & Pinedo, H. M. (1995). *Camptothecins: New anticancer agents*. USA: CRC Press.

Ren, Y., Picout, D. R., Ellis, P. R., Ross-Murphy, S. B., & Reid, J. S. G. (2005). A novel xyloglucan from seeds of *Afzelia africana* Se. Pers.—Extraction, characterization, and conformational properties. *Carbohydrate Research*, *340*, 997–1005.

Ribeiro, C., Arizaga, G. G. C., Wypych, F., & Sierakowski, M.-R. (2008). Nanocomposites coated with xyloglucan for drug delivery: In vitro studies. *International Journal of Pharmaceutics*, *367*, 204–210.

Schoeler, B., Deloreme, N., Doench, I., Sukhorukov, G. B., Fery, A., & Glinel, K. (2006). Polyelectrolite films based on polysaccharides of different conformations: Effect on multilayer structure and mechanical properties. *Biomacromolecules*, *7*, 2065–2071.

Shenderova, A., Burke, T. G., & Schwendeman, S. P. (1997). Stabilization of 10 hydroxycamptothecin in poly(lactide-co-glycolide) microsphere delivery vehicles. *Pharmaceutical Research*, *14*, 1406–1413.

Shenderova, A., Burke, T. G., & Schwendeman, S. P. (1999). The acidic microclimate in poly(lactide-co-glycolid) microspheres stabilizes camptothecins. *Pharmaceutical Research*, *16*, 241–248.

Shirakawa, M., Yamotoya, K., & Nishinari, K. (1998). Tailoring of xyloglucan properties using an enzyme. *Food Hydrocolloid*, *12*, 25–28.

Siepmann, J., & Peppas, N. A. (2001). Modeling of drug release from delivery systems based on hydroxypropyl methylcellulose (HPMC). *Advanced Drug Delivery Reviews*, *48*, 139–157.

Sierakowski, M.-R., Castro, L. B. R., Lucyszyn, N., & Petri, D. F. S. (2007). Assembling of xyloglucan and lectin onto Si wafers and onto amino-terminated surfaces. *Journal of Brazilian Chemical Society*, *18*, 1017–1023.

Silva, R. A., Carmona-Ribeiro, A.-M., & Petri, D. F. S. (2007). Adsorption behavior and activity of horseradish peroxidase onto polysaccharide-decorated particles. *International Journal of Biological Macromolecules*, *41*, 404–409.

Sims, I. M., Gane, A. M., Dunstan, D., Allan, G. C., Boger, D. V., Melton, L. D., et al. (1998). Rheological properties of xyloglucans from different plant species. *Carbohydrate Polymers*, *37*, 61–69.

Storm, P. B., Moriarity, J. L., Tyler, B., Burger, P. C., Brem, H., & Weingart, J. (2002). Polymer delivery of camptothecin against 9L gliosarcoma: Release, distribution, and efficacy. *Journal of Neuro-Oncology*, *56*, 209–217.

Stupp, T., Freitas, R. A., Sierakowski, M.-R., Deschamps, F. C., Wisniewski, A., Jr., & Biavatti, M. W. (2008). Characterization and potential uses of *Copaifera langsdorfii* seeds and seed oil. *Bioresource Technology*, *99*, 2659–2663.

Suisha, F., Kawasaki, N., Miyazaki, S., Shirakawa, M., Yamatoya, K., Sasaki, M., et al. (1998). Xyloglucan gels as sustained release vehicles for the intraperitoneal administration of mitomycin C. *International Journal of Pharmaceutics*, *172*, 27–32.

Synytsya, A., Synytsya, A., Blafkova, P., Volka, K., & Král, V. (2007). Interaction of meso-tetrakis(4-ulphonatophenyl)porphine with chitosan in aqueous solutions. *Spectrochimica Acta A*, *66*, 225–235.

Takahashi, A., Suzuki, S., Kawasaki, N., Kubo, W., Miyazaki, S., Loebenberg, R., et al. (2002). Percutaneous absorption of non-steroidal anti-inflammatory drugs from in situ gelling xyloglucan formulations in rats. *International Journal of Pharmaceutics*, *246*, 179–186.

Takimoto, C. H., Wright, J., & Arbuck, S. G. (1998). Clinical applications of the camptothecins. *Biochimica et Biophysica Acta*, *1400*, 107–119.

Ueta, R. R., & Diniz, F. B. (2008). Adsorption of concanavalin A and lentil lectin on platinum electrodes followed by electrochemical impedance spectroscopy: Effect of protein state. *Colloids and Surfaces B*, *61*, 244–249.

Varner, J. E., & Lin, L.-S. (1989). Plant cell wall architecture. *Cell*, *56*, 231–239.

Vieira, N. A. B., Moscardini, M. S., Tiera, V. A. O., & Tiera, M. J. (2003). Aggregation behavior of hydrophobically modified dextran in aqueous solution: A fluorescence probe study. *Carbohydrate Polymers*, *53*, 137–143.

Wall, M. E., Wani, M. C., Cook, C. E., Palmer, K. H., McPhail, A. T., & Sim, G. A. (1966). Plant antitumor agents. I. The isolation and structure of camptothecin, a novel alkaloidal leukemia and tumor inhibitor from *Camptotheca acuminata*. *Journal of the American Chemical Society*, *88*, 3888–3890.

Wang, Q., Ellis, P. R., Ross-Murphy, S. B., & Reid, J. S. G. (1996). A new polysaccharide from a traditional Nigerian plant food: *Detarium senegalense* Gmelin. *Carbohydrate Research*, *284*, 229–239.

Watanabe, M., Kawano, K., Yokoyama, M., Opanasopit, P., Okano, T., & Maitani, Y. (2006). Preparation of camptothecin-loaded polymeric micelles and evaluation of their incorporation and circulation stability. *International Journal of Pharmaceutics*, *308*, 183–189.

Xiong, X. Y., Tam, K. C., & Gan, L. H. (2005). Release kinetics of hydrophobic and hydrophilic model drugs from pluronic F127/poly(lactic acid) nanoparticles. *Journal of Controlled Release*, *103*, 73–82.

Yamanaka, S., Yuguchi, Y., Urakawa, H., Kajiwara, K., Shirakawa, M., & Yamatoya, K. (2000). Gelation of tamarind seed polysaccharide xyloglucan in the presence of ethanol. *Food Hydrocolloids*, *14*, 125–128.

Yoo, M. K., Choi, H. K., Kim, T. H., Choi, Y. J., Akaike, T., Shirakawa, M., et al. (2005). Drug release from xyloglucan beads coated with Eudragit for oral drug delivery. *Archives of Pharmacal Research*, *28*, 736–742.

York, W. S., Kumar-Kolli, V. S., Orlando, R., Albersheim, P., & Darvill, A. G. (1996). The structures of arabinoxyloglucans produced by solanaceous plants. *Carbohydrate Research*, *285*, 99–128.

Zhang, H., Zou, K., Guo, S., & Duan, D. (2006). Nanostructural drug-inorganic clay composites: Structure, thermal property and in vitro release of captopril-intercalated Mg–Al-layered double hydroxides. *Journal of Solid State Chemistry*, *179*, 1792–1801.

Zuleger, S., & Lippold, B. C. (2001). Polymer particle erosion controlling drug release. I. Factors influencing drug release and characterization of the release mechanism. *International Journal of Pharmaceutics*, *217*, 139–152.